AIP | Review of Scientific Instruments

A technique for continuous measurement of the quality factor of mechanical oscillators

Nicolás D. Smith

Citation: Review of Scientific Instruments **86**, 053907 (2015); doi: 10.1063/1.4920922
View online: http://dx.doi.org/10.1063/1.4920922
View Table of Contents: http://scitation.aip.org/content/aip/journal/rsi/86/5?ver=pdfcov
Published by the AIP Publishing

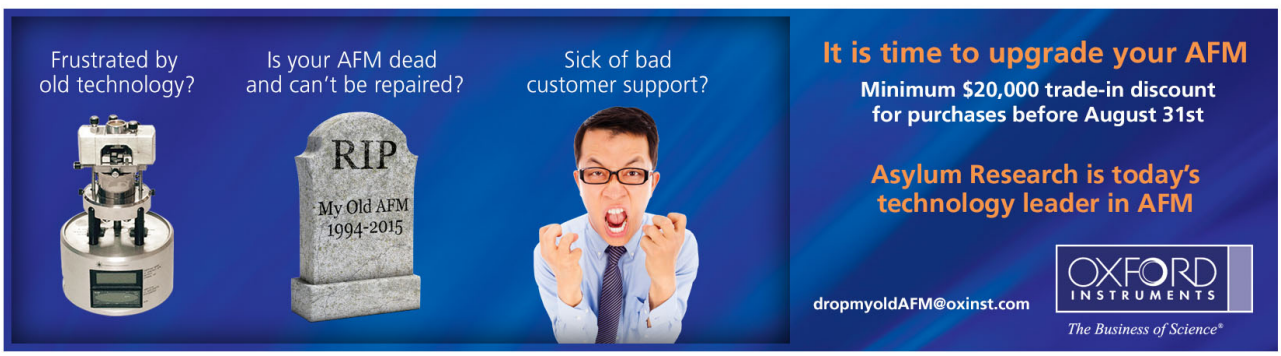

A technique for continuous measurement of the quality factor of mechanical oscillators

Nicolás D. Smith
LIGO Laboratory, California Institute of Technology, Pasadena, California 91125, USA

(Received 8 January 2015; accepted 29 April 2015; published online 15 May 2015)

Thermal noise is a limit to precision measurement in many fields. The relationship of the quality factor of mechanical systems to the thermal noise has compelled many researchers to search for materials with low mechanical losses. Typical measurements of mechanical quality factor involve exciting a mechanical resonator and observing the exponential decay of the amplitude under free oscillations. Estimation of the decay time allows one to infer the quality factor. In this article, we describe an alternative technique in which the resonator is forced to oscillate at constant amplitude, and the quality factor is estimated by measuring the drive amplitude required to maintain constant oscillation amplitude. A straightforward method for calibration of the quality factor is presented, along with an analysis of the propagation of measurement uncertainties. Such a technique allows the quality factor to be measured continuously in real time and at constant signal to noise ratio. [http://dx.doi.org/10.1063/1.4920922]

I. INTRODUCTION

Thermal noise is of particular importance in mechanical systems used in precision measurement applications, such as gravitational-wave detection,[1] optical clocks,[2] and micromechanical resonators.[3] The measurement precision of such systems is often limited by thermal fluctuations of the mechanical components. The quality factor of a mechanical system characterizes the tendency for the system to maintain energy under free oscillations. A system with a high quality factor dissipates only a small amount of energy during one oscillation and thus is well isolated from the environment. According to the fluctuation-dissipation relationship, the noise spectral density of thermal fluctuations scales inversely with the quality factor.[4,5] Thus, researchers in these fields extensively studied the quality factor of various materials used in these experiments.[5–11] The related concept of decoherence in quantum mechanical systems also drives researchers of hybrid quantum systems,[12] macroscopic quantum mechanics,[13] cavity opto-mechanics,[14] and superfluid opto-mechanics[15] to design and explore systems with high quality factors.

Current state-of-the-art methods to measure mechanical quality factor involve a resonant mechanical system which is driven at the resonance frequency, then the drive signal is removed and the system is allowed to experience free oscillations. Mechanical losses cause the oscillation amplitude to exponentially decay with a 1/e amplitude decay time constant proportional to the quality factor. A curve fitting analysis of the decaying exponential function allows parameter estimation of the quality factor.[8]

In this article, we describe an alternative technique in which the resonator is forced to oscillate at fixed amplitude. The energy supplied to the resonator to maintain fixed amplitude oscillation must be equal to the energy dissipated; thus, the drive amplitude provides a measure of the mechanical loss.

Using a self resonating circuit in an open-loop configuration has been shown previously.[16] In addition, this technique is similar to the one used in non-contact atomic force microscopy where a cantilever is set to resonate at constant amplitude, and shifts of the cantilever resonant frequency as the cantilever position is scanned over a structure are used to construct an image of the structure.[17] However, the analysis of loop response, calibration into physical parameters, and noise characteristics of the dissipation signal have not before been presented in the literature.

II. A HARMONIC OSCILLATOR DRIVEN NEAR RESONANCE

For a resonant system, the quality factor, Q, is defined as the resonance frequency divided by the full width half maximum of the resonance in frequency space. For mechanical systems, this is closely related to the loss angle of the mechanical restoring force, ϕ. These are also closely related to the characteristic ring-down time of the resonator.

The quality factor is related to the loss angle by

$$Q = \phi^{-1} = \frac{\omega_0 \tau}{2}, \tag{1}$$

where Q is the quality factor, ϕ is the loss angle, ω_0 is the resonant angular frequency, and τ is the ring-down time constant. This expression is valid when $\phi \ll 1$.

We will refer to the system of interest as the oscillator under test (OUT). The equation of motion for the OUT is the differential equation for a driven simple harmonic oscillator,

$$\ddot{\mathrm{x}} = -\omega_0^2(1 + i\phi)\mathrm{x} + \mathrm{f}, \tag{2}$$

where x is the position, f is the driving force per unit mass, ω_0 is the natural frequency, and ϕ is the loss angle. The choice of a frequency independent ϕ is referred to as structural loss, but in general ϕ may have a frequency dependence.

The linearity of the equation of motion allows us to consider periodic motion of different frequencies separately.

We will consider motion happening at frequencies close to ω_0, such that $\mathrm{x} = x\mathrm{e}^{-i\Omega t}$, $\mathrm{f} = f\mathrm{e}^{-i(\Omega t-\delta)}$, and $\Omega = \omega_0 + \omega$, where $\omega \ll \omega_0$. Thus, we will concentrate on the amplitude envelope variables x and f while removing the high frequency oscillating part. We include δ as an explicit phase shift of the force. Note that in this convention, the resonance frequency occurs at $\omega = 0$, and that ω may take negative values that still correspond to physical solutions. Thus from (2), we have

$$\begin{aligned} -(\omega_0+\omega)^2 x &= -\omega_0^2(1+i\phi)x + f\mathrm{e}^{i\delta}, \\ -(\omega_0^2 + 2\omega_0\omega)x &= -\omega_0^2(1+i\phi)x + f\mathrm{e}^{i\delta}, \\ \frac{x}{f} &= \frac{-i\mathrm{e}^{i\delta}}{\phi\omega_0^2}\frac{1}{1+i\frac{2\omega}{\phi\omega_0}}, \end{aligned} \tag{3}$$

where in the second line, the term that is second order in ω/ω_0 has been neglected.

Thus, for a periodic driving force on resonance (i.e., at $\omega = 0$), the ratio of the amplitude of motion to the drive amplitude is inversely proportional to the loss angle, ϕ. As the system achieves steady state, the energy dissipated in the oscillator must be exactly canceled by the energy supplied by the driving force. It is this feature that is the basis of technique described here. We also see that the transfer function from drive amplitude to the amplitude of motion is characterized by a single pole; the impulse response of the system is, as expected, an exponential function with time constant $\tau = \frac{2}{\phi\omega_0}$.

III. CALIBRATED MEASUREMENT OF THE QUALITY FACTOR USING AN AMPLITUDE LOCKED LOOP (ALL)

In Sec. II, we showed that, on resonance, the ratio of the motion to the drive amplitude provides a measure of the loss angle once the system has achieved steady state. However, there are practical issues in making such a measurement. The first is the assumption that the drive force is periodic with a frequency exactly equal to the natural frequency of the oscillator. This is difficult in practice because in order to drive the oscillator coherently at the response peak, the drive frequency must be matched to the natural frequency to a precision of one part in $1/\phi$. The second practical issue is that once the drive is engaged, one must wait for the system to approach steady state equilibrium, the scale of which is set by τ, which may be a long time.

These two practical problems may be solved with a pair of control systems, the first designed to keep the driving force always locked to the natural resonant frequency of the oscillator and the second to force the oscillator to quickly approach, and then maintain, a fixed and chosen amplitude of motion. The controls systems are shown schematically in Figure 1.

In order to drive the oscillator at the correct frequency, we will produce an auxiliary oscillation signal that is derived from the position signal. This auxiliary oscillator must have a fixed amplitude and have a fixed phase offset, δ, relative to the measured position signal. By virtue of the constant phase offset, the auxiliary oscillator frequency is matched to the natural frequency of the OUT. One method to produce such a auxiliary oscillator is with a phase locked loop where the auxiliary oscillator is a voltage controlled oscillator and

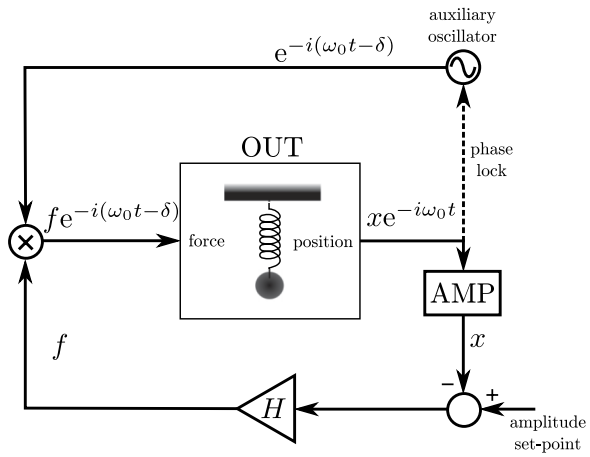

FIG. 1. Block diagram of the driving system. The oscillator under test (OUT) is driven by an auxiliary oscillator phase referenced to the position signal. The amplitude is determined using an amplitude detector, labeled AMP. The amplitude is controlled by an ALL.

locked to the OUT position oscillation signal. Another method is to take the OUT position signal, perform a narrow band-pass filter around ω_0, then use a hard-limiter to produce a fixed amplitude square wave, and again band-pass to finally have a fixed amplitude sine wave, and an additional filter may be used to set the desired value for δ. For maximum response, $\delta = \pi/2$.

With the goal of forcing the OUT to oscillate at a fixed amplitude, we employ an ALL system.[18] Such a system comprises an amplitude detector, this is compared to a reference amplitude to produce an error signal and then is amplified and then used to control the magnitude of the driving force. The amplitude detector may be a band-limited rms detector centered at ω_0.

We shall consider a linearized model of the ALL (shown in Figure 2) in order to analyze the closed loop response of the system. The plant of the system P will be represented by a filter which represents the natural response of the OUT position amplitude, x, given a driving force, f,

$$P \equiv \frac{x}{f} = \frac{1}{\phi\omega_0^2}\frac{1}{1+i\tau\omega}, \tag{4}$$

where we have set the drive oscillator phase $\delta = \pi/2$. The blocks S and A represent the sensor and actuator gains, respectively. We begin by assuming these are unknown, i.e., our actuator and sensor are uncalibrated, but that their frequency response is flat near the resonance frequency. H is our feedback gain. The open loop gain is defined as $G = HAPS$.

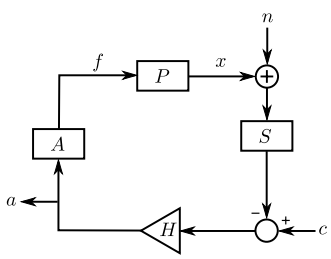

FIG. 2. Linearized model of the amplitude locked loop.

We may examine the frequency response of the OUT amplitude to changes in the ALL set-point,

$$\frac{x}{c} = \frac{HAP}{1+G} = \frac{HA}{\omega_0\left(\phi\omega_0 + \frac{SHA}{\omega_0}\right)\left(1 + \frac{2i\omega}{\phi\omega_0 + \frac{SHA}{\omega_0}}\right)},$$

where c is the amplitude set-point. If we take the limit where the open loop gain is high (explained below), this simplifies to

$$\frac{x}{c} = \frac{1}{S\left(1 + \frac{i\omega}{\omega_U}\right)}, \tag{5}$$

where ω_U is the unity gain frequency (UGF) of the ALL and is derived in Appendix A. The high gain limit is satisfied when the UGF of the loop is much larger than $1/\tau$. The time scale for the ALL to come to equilibrium is defined by the UGF. The amplitude will approach $x = c/S$ with an exponential decay having a time constant equal to $1/\omega_U$, which is easily controlled by changing the feedback gain, H. Thus, the response of the system can be made much faster than the natural time constant, τ. Note that for the system to be stable, it is sufficient for H to be a frequency independent gain because the plant acts as a single pole low-pass filter. However, in order to null the mean error of the system, it is beneficial for H to act as an integrator at some frequency below the UGF, though this does not significantly change the closed loop frequency response.

We have so far described a system which forces the OUT to quickly approach some fixed oscillation amplitude and maintain that amplitude in dynamic equilibrium. When in equilibrium, the energy provided by the driving force is balanced by the energy dissipated internally in the OUT. Therefore, the control output of H, labeled a in Figure 2, is a measurement of ϕ once it has been properly calibrated. This can be seen by as follows:

$$\frac{a}{c} = \frac{H}{1+G} = \frac{H\phi\omega_0(1+i\tau\omega)}{\left(\phi\omega_0 + \frac{SHA}{\omega_0}\right)\left(1 + \frac{2i\omega}{\phi\omega_0 + \frac{SHA}{\omega_0}}\right)},$$

and again after, we take the limit of high gain,

$$\frac{a}{c} = \frac{\phi\omega_0 H_U(1+i\tau\omega)}{2\omega_U\left(1 + \frac{i\omega}{\omega_U}\right)}, \tag{6}$$

where H_U is the feedback gain evaluated at the UGF. If we take the time average ($\omega = 0$), and solve for ϕ, we have

$$\phi = Q^{-1} = \frac{2\omega_U}{cH_U\omega_0}\langle a\rangle, \tag{7}$$

where the angle brackets indicate a time average. This expression shows that the signal a may be calibrated in terms of H and c, which are parameters of the ALL, as well as the two frequencies ω_0 and ω_U which are straightforward to measure. This shows that a measurement of the UGF of the ALL is in effect a calibration of both the unknown actuator and sensor gains A and S. There is no need to have an absolute calibration of the sensor in meters, nor the actuator in Newtons.

IV. SIGNAL TO NOISE RATIO (SNR)

As shown in Eq. (7), the physical quantity ϕ is determined by measuring the mean value of the control signal, $\langle a\rangle$. In order to quantify the precision of such a measurement, we define the SNR, ρ_y for determination of the mean value for a signal y to be

$$\rho_y \equiv \frac{\langle y\rangle}{\sqrt{\int_0^\infty \mathrm{N}_y\left(\frac{1}{1+(\tau_{avg}\omega)^2}\right)^2\frac{d\omega}{2\pi}}}, \tag{8}$$

where N_y is the noise power spectral density measured in the signal y, and τ_{avg} is the time scale of a *second order* averaging low pass filter. The integral in the denominator is formally taken to $\omega \to \infty$, though the low pass filter is intended to make the contribution of noise at frequencies higher than τ_{avg}^{-1} negligible, as long as the noise power rises no steeper than ω^2.

If we assume the sensing noise of the oscillator around ω_0 is frequency independent, with a noise power spectral density, N_x (injected at the point n in Figure 2), then the open-loop SNR of the measurement of the oscillator amplitude, x, is

$$\rho_x = \langle x\rangle\sqrt{\frac{8\tau_{avg}}{\mathrm{N}_x}}, \tag{9}$$

where, as expected, the SNR increases as the square root of the averaging time.

Propagation of the sensing noise in x to the control signal a gives

$$\mathrm{N}_a = \mathrm{N}_x\left|\frac{SH}{1+G}\right|^2 = \mathrm{N}_x\left|\frac{SH(1+i\tau\omega)}{\left(1+\frac{i\omega}{\omega_U}\right)}\right|^2. \tag{10}$$

Here, we see that the closed loop response works as an effective differentiating filter at frequencies between τ^{-1} and ω_U. Thus, a second order low pass filter is necessary to bound the high frequency noise contribution and is the reason for a second order low pass filter in Eq. (8). An algorithm for second order filtering of an arbitrary length data stream is given in Appendix B.

With the noise given in (10), along with Eqs. (8) and (9), we may calculate the SNR in the measurement of ϕ to be

$$\rho_\phi = \frac{\rho_x}{\sqrt{1+\frac{\tau^2}{\tau_{avg}^2}}}, \tag{11}$$

where we have taken the limit where $\omega_U \gg \tau_{avg}^{-1}$, or that the averaging time is long compared to the loop response time. Equation (11) shows that for averaging times longer than the ring-down time, the SNR of the measurement of ϕ is approximately the open-loop SNR of x. While for averaging times less than the ring-down time, the SNR of ϕ compared to x is reduced by the ratio τ_{avg}/τ.

V. COMPARISON OF THE CONTINUOUS TECHNIQUE AND THE RING-DOWN TECHNIQUE

The steady state nature of the technique described in this article gives it several benefits when compared to the conventional ring-down technique.

Because the oscillator is maintained at constant amplitude, the signal to noise ratio of the measurement is constant. This is in contrast to the ring-down technique, where the oscillator amplitude decays and the SNR is correspondingly reduced.

In the case of a ring-down measurement, to make a single estimate of the ring-down time, it is typical for the measurement duration to be one or more times the ring-down time. In some experiments, the ring down time may be as long as two years.[19] In principle, the ring-down time may be estimated in less time than this, but having an estimation of the measurement precision is non-trivial. In the case of a continuous measurement, it is possible to make estimates of ϕ in less time than τ, and the precision is simply set by Eq. (11). For example, if one desires an estimate of ϕ in a time $\tau/10$, they know that the measurement SNR of ϕ will have a SNR that is 10 times less than the SNR of x measured over the same time scale.

Conversely, one may also make measurements which have a duration many times the ring-down time. In the case of a ring-down measurement, this would require a periodic ring up of the oscillator and a combination of several ring-down measurements. In the continuous case, the signal may be averaged for any duration, with the corresponding improvement of the SNR over time.

Using the continuous technique, it is possible to determine of the dependence of ϕ on other parameters (for example, temperature[20]) in a continuous way. It is necessary that the sweep time scale be slower than the averaging time scale. It also may be important to correct for variation in the sensing or actuation gain by monitoring or controlling the UGF of the ALL.

Some systems show a nonlinearity in the form of an amplitude dependent loss angle.[21,22] Measurements of the ring-down of these systems will have multiple decay times, which complicates curve fitting of the ring-down signal. The continuous measurement occurs at a constant amplitude and thus will measure the loss angle of only this amplitude. In fact, several measurements can be made where the amplitude set-point may be varied in order to systematically determine the dependence of ϕ on amplitude with high SNR.

Finally, the continuous measurement allows for a system with several resonant modes to have the loss angle of multiple modes measured simultaneously, with the requirement that the mode frequency separation is much larger than the ALL UGFs. It is also possible, in principle, to measure multiple modes using a conventional ring-down technique, though the data processing is non-trivial, and the measurement time is constrained by the mode with the longest decay time constant.

There are also drawbacks of this technique compared to the ring-down technique. The resonant frequency and UGF are used in calibration of the quality factor measurement, and measurement of these frequencies may introduce systematic errors. In addition, the relative complexity of this system is considerably increased compared to a ring-down measurement. Finally, this technique requires that the actuator is used during measurement, where in the ring-down technique, the actuator may be disabled after first exciting the oscillation. It is possible that the actuator may introduce damping which will introduce a systematic error in the quality factor measurement.

VI. EXPERIMENTAL DEMONSTRATION

This technique was demonstrated with a silicon resonator in a vacuum system. The dissipation of the resonator is far higher than the material limits and is likely dominated by loss in the clamp. The resonator was driven by an electrostatic actuator with 1 kV bias voltage and 0-100 V drive signal. The motion of the resonator was read out with a helium neon laser reflected from the resonator and detected on quadrant photodetector. The resonator is a silicon cantilever clamped between two pieces of steel. It has dimensions of $35 \times 5 \times 0.3$ mm and a fundamental resonant frequency of 247.5 Hz. The control system was implemented on an Advanced LIGO custom real-time digital control system sampled at 16 kHz. A logical block diagram of the controller is given in Figure 3. The amplitude detector was realized by means of a band limited rms filter centered at the resonant frequency. The auxiliary oscillator was derived by first band-passing the resonator signal, then applying a differentiation filter (to set $\delta = \pi/2$), saturating the signal to create a fixed amplitude square wave, then band-passing again to produce a fixed amplitude sine wave. The net effect is a fixed amplitude sine wave which has a phase offset of $\delta = \pi/2$ relative to the resonator readout. The ALL had a UGF of 6.2 ± 0.3 Hz.

Figure 4 shows the behavior of the system when the feedback is engaged, the set-point c is changed, and finally,

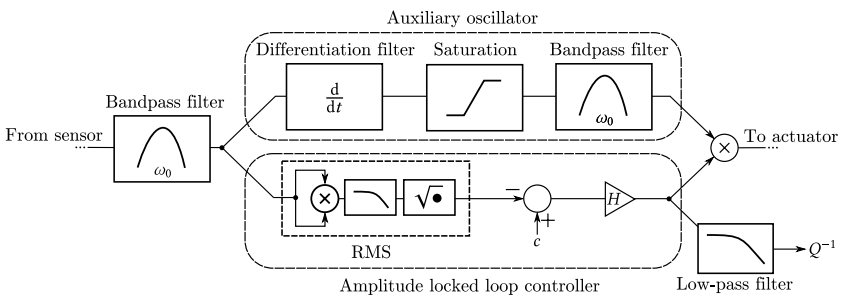

FIG. 3. Implementation of continuous quality factor measurement in a digital control system. Description of each component is included in the text.

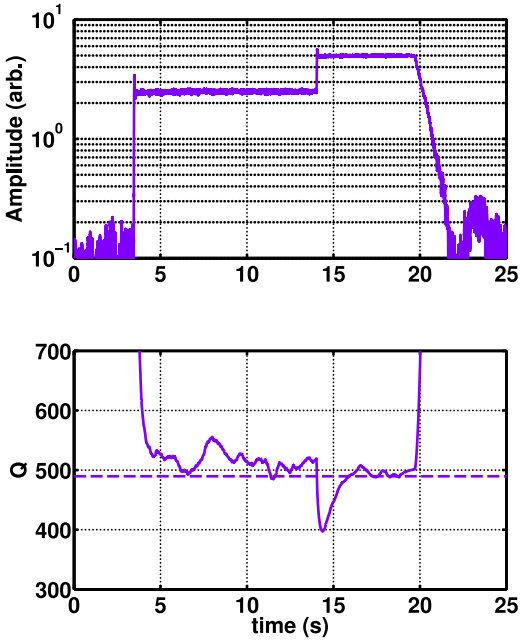

FIG. 4. The top axes show the time series of the oscillator amplitude, the bottom axes show the real-time quality factor calculation including a 2 s averaging filter. At 3.5 s, the feedback system is engaged. At 14.6 s, the set-point amplitude is changed to a higher value. At 19.7 s, the feedback is disabled and the system experiences free exponential ring-down. A curve fit of the ring-down gives quality factor value of $Q = 489 \pm 5$. This value is indicated as a dashed line on the bottom axes.

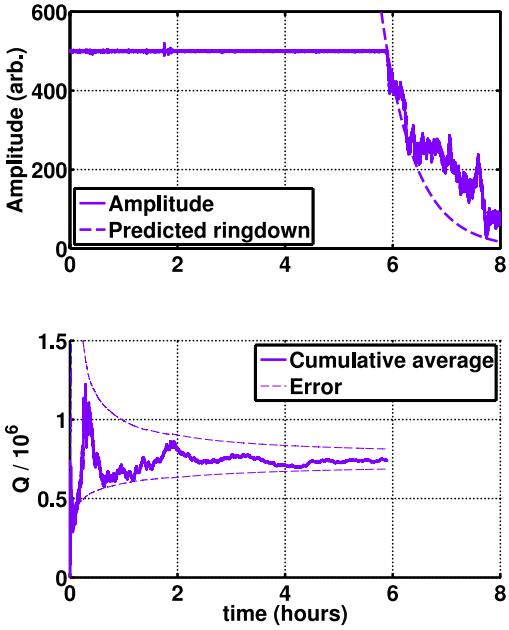

FIG. 5. The Q of a silicon cantilever is measured using the continuous technique. The top axes show the oscillator amplitude held at a constant value before the feedback is disengaged. A cumulative average of the Q measurement is shown on the bottom axes. One can see how the signal to noise ratio is improved over time. The free ringdown as predicted by the continuous Q measurement is also shown on the top axes. However, the energy of the system is quickly dominated by environmental excitations after the feedback system is disengaged, making a ring-down measurement impractical in this case. This is an example of a system which benefits from the use of the continuous technique.

the feedback is disabled. The system shows the characteristic exponential ring-down after the feedback is disabled. Also shown is the output of the real-time quality factor computation, the uncertainty of the UGF measurement introduces a systematic calibration error. In this case, the error is 5%. It is also clear that there is an additional systematic uncertainty which is reduced as the oscillator amplitude is increased. In the high amplitude region, given the uncertainties, there is a good agreement between the real-time quality factor calculation and the result of a curve fit of the exponential ring-down.

A second system is shown in Figure 5. This system is a silicon cantilever cooled to 95 K. The cantilever has dimensions $34 \times 5 \times 0.92$ mm with a resonant frequency of 106.1 Hz. The vacuum system, cantilever readout, and actuator are the same as the system described above. The ALL was tuned to a 3.5 Hz UGF. The Q of this system was measured to be $(7.5 \pm 0.6) \times 10^5$, which corresponds to a ring-down time of 0.6 h. The figure shows the output of a cumulative average of the calibrated quality factor measurement over time. Also shown is the cumulative standard deviation of the mean of the data points centered about the final measured value, after the data were decimated to a sample rate below that of the ALL UGF. The fixed amplitude setpoint of this system was chosen to be a factor of two below where the readout showed significant nonlinear compression of the amplitude signal. This amplitude was only a factor of a few above the typical amplitude of the system when under the influence of environmental excitations only. One may see that the free ringdown of the system is quickly dominated by environmental excitations, though the early ringdown is qualitatively consistent with the prediction given by the continuous Q measurement. This type of system, where the maximum desired amplitude is not much larger than the amplitude of background excitations, is an ideal system to take advantage of the continuous measurement technique. A ringdown measurement is impractical because the system will too quickly become dominated by the influence of the environment, but the continuous technique is able to perform long time scale measurements (compared to the ringdown time) and accumulate SNR over the entire measurement.

VII. CONCLUSION

We have described a technique for real-time continuous measurement of the quality factor of mechanical systems by means of a feedback system. We have demonstrated the technique on a pair of systems, each of which shows different features of the technique. This technique holds promise to increase measurement precision and efficiency of quality factor measurements and may aid in the materials research required to investigate low-loss materials for precision measurement experiments.

ACKNOWLEDGMENTS

The author would like to thank Koji Arai, W. Zach Korth, Tobin Fricke, Yuta Michimura, Matthew Abernathy, and Lisa Barsotti for useful discussions and comments, and Shiuh Chao for providing one of the silicon resonators used in this article. LIGO was constructed by the California Institute of Technology and Massachusetts Institute of Technology with

funding from the National Science Foundation and operates under Cooperative Agreement No. PHY-0757058. This paper carries LIGO Document No. LIGO-P1400183.

APPENDIX A: THE UNITY GAIN FREQUENCY OF THE ALL

An important quantity of any feedback control system is the UGF. It is the frequency when the open loop gain of the system has unity magnitude. For our ALL, the UGF, ω_{U}, is

$$|G(\omega_{\mathrm{U}})| = 1,$$
$$\frac{|SH_{\mathrm{U}}A|}{\omega_0^2\phi}\left|\frac{1}{1+\frac{i2\omega_{\mathrm{U}}}{\phi\omega_0}}\right| = 1,$$
$$\omega_{\mathrm{U}} = \frac{1}{2}\sqrt{\frac{|SH_{\mathrm{U}}A|^2}{\omega_0^2} - \phi^2\omega_0^2},$$

where we have defined H_{U} to be the gain of H evaluated at the UGF. The size of the $\phi\omega_0$ correction is small, so in the limit when the open loop gain is high,

$$\omega_{\mathrm{U}} = \frac{|SH_{\mathrm{U}}A|}{2\omega_0}. \tag{A1}$$

This frequency sets the time scale for the closed loop ALL system to come to equilibrium.

APPENDIX B: SECOND ORDER AVERAGING OF ALL MEASUREMENT SAMPLES

Section III suggests the use of a second-order low-pass filter to remove sensing noise and estimate the mean value of the control signal. However, using such a filter has the possibly undesirable feature that older measurement samples are essentially forgotten by the filter for times longer than the filter settling time. Here, we describe an algorithm which maintains memory of all measurement samples but still has the characteristic of a second order low pass filter.

Given a set of measurement samples $\{x_i\}$, the mean value after n samples is

$$a_n = \frac{n-1}{n}a_{n-1} + \frac{x_n}{n}, \tag{B1}$$

where a_{n-1} is defined recursively and is the mean of the first $n-1$ samples. This is approximately a first order low-pass filter of the data. To obtain a second order low pass, we may apply the formula again to the samples $\{a_i\}$,

$$d_n = \frac{n-1}{n}d_{n-1} + \frac{a_n}{n}. \tag{B2}$$

Combining the two previous formulae gives

$$d_n = \frac{(2n-1)(n-1)}{n^2}d_{n-1} - \frac{(n-1)(n-2)}{n^2}d_{n-2} + \frac{x_n}{n^2}. \tag{B3}$$

This gives an appropriate second order low passed estimate of the mean value, where all measurement samples are included.

[1]P. R. Saulson, "Thermal noise in mechanical experiments," Phys. Rev. D **42**, 2437–2445 (1990).
[2]T. Kessler, C. Hagemann, C. Grebing, T. Legero, U. Sterr, F. Riehle, M. J. Martin, L. Chen, and J. Ye, "A sub-40-MHz-linewidth laser based on a silicon single-crystal optical cavity," Nat. Photonics **6**(10), 687–692 (2012).
[3]T. H. Stievater, W. S. Rabinovich, N. A. Papanicolaou, R. Bass, and J. B. Boos, "Measured limits of detection based on thermal-mechanical frequency noise in micromechanical sensors," Appl. Phys. Lett. **90**(5), 051114 (2007).
[4]H. B. Callen and T. A. Welton, "Irreversibility and generalized noise," Phys. Rev. **83**, 34–40 (1951).
[5]P. Amico, L. Bosi, L. Carbone, L. Gammaitoni, F. Marchesoni, M. Punturo, F. Travasso, and H. Vocca, "Mechanical quality factor of large mirror substrates for gravitational waves detectors," Rev. Sci. Instrum. **73**(1), 179 (2002).
[6]T. Uchiyama, T. Tomaru, M. E. Tobar, D. Tatsumi, S. Miyoki, M. Ohashi, K. Kuroda, T. Suzuki, N. Sato, T. Haruyama, A. Yamamoto, and T. Shintomi, "Mechanical quality factor of a cryogenic sapphire test mass for gravitational wave detectors," Phys. Lett. A **261**(12), 5–11 (1999).
[7]S. Nietzsche, R. Nawrodt, A. Zimmer, R. Schnabel, W. Vodel, and P. Seidel, "Cryogenic q-factor measurement of optical substrates for optimization of gravitational wave detectors," Supercond. Sci. Technol. **19**(5), S293 (2006).
[8]R. Nawrodt, A. Zimmer, T. Koettig, C. Schwarz, D. Heinert, M. Hudl, R. Neubert, M. Thürk, S. Nietzsche, W. Vodel, P. Seidel, and A. Tünnermann, "High mechanical Q-factor measurements on silicon bulk samples," J. Phys.: Conf. Ser. **122**(1), 012008 (2008).
[9]G. M. Harry, A. M. Gretarsson, P. R. Saulson, S. E. Kittelberger, S. D. Penn, W. J. Startin, S. Rowan, M. M. Fejer, D. R. M. Crooks, G. Cagnoli, J. Hough, and N. Nakagawa, "Thermal noise in interferometric gravitational wave detectors due to dielectric optical coatings," Classical Quantum Gravity **19**(5), 897 (2002).
[10]S. D. Penn, P. H. Sneddon, H. Armandula, J. C. Betzwieser, G. Cagnoli, J. Camp, D. R. M. Crooks, M. M. Fejer, A. M. Gretarsson, G. M. Harry, J. Hough, S. E. Kittelberger, M. J. Mortonson, R. Route, S. Rowan, and C. C. Vassiliou, "Mechanical loss in tantala/silica dielectric mirror coatings," Classical Quantum Gravity **20**(13), 2917 (2003).
[11]A. Borrielli, M. Bonaldi, E. Serra, A. Bagolini, and L. Conti, "Wideband mechanical response of a high-q silicon double-paddle oscillator," J. Micromech. Microeng. **21**(6), 065019 (2011).
[12]M. Goryachev, D. L. Creedon, E. N. Ivanov, S. Galliou, R. Bourquin, and M. E. Tobar, "Extremely low-loss acoustic phonons in a quartz bulk acoustic wave resonator at millikelvin temperature," Appl. Phys. Lett. **100**(24), 243504 (2012).
[13]Y. Chen, "Macroscopic quantum mechanics: Theory and experimental concepts of optomechanics," J. Phys. B: At., Mol. Opt. Phys. **46**(10), 104001 (2013).
[14]M. Aspelmeyer, T. J. Kippenberg, and F. Marquardt, *Cavity Optomechanics*, e-print arXiv:1303.0733.
[15]L. A. De Lorenzo and K. C. Schwab, "Superfluid optomechanics: Coupling of a superfluid to a superconducting condensate," New J. Phys. **16**(11), 113020 (2014).
[16]R. N. Kleiman, G. K. Kaminsky, J. D. Reppy, R. Pindak, and D. J. Bishop, "Single-crystal silicon high-q torsional oscillators," Rev. Sci. Instrum. **56**(11), 2088 (1985).
[17]T. R. Albrecht, P. Grütter, D. Horne, and D. Rugar, "Frequency modulation detection using high-Q cantilevers for enhanced force microscope sensitivity," J. Appl. Phys. **69**(2), 668 (1991).
[18]T. J. Moir, "Analysis of an amplitude-locked loop," Electron. Lett. **31**(9), 694–695 (1995).
[19]K. Tokmakov, V. Mitrofanov, V. Braginsky, S. Rowan, and J. Hough, "Bifilar pendulum mode Q factor for silicate bonded pendulum," AIP Conf. Proc. **523**(1), 445–446 (2000).
[20]R. Nawrodt, C. Schwarz, S. Kroker, I. W. Martin, R. Bassiri, F. Brückner, L. Cunningham, G. D. Hammond, D. Heinert, J. Hough, T. Käsebier, E.-B Kley, R. Neubert, S. Reid, S. Rowan, P. Seidel, and A. Tünnermann, "Investigation of mechanical losses of thin silicon flexures at low temperatures," Classical Quantum Gravity **30**(11), 115008 (2013).
[21]Y. L. Huang and P. R. Saulson, "Dissipation mechanisms in pendulums and their implications for gravitational wave interferometers," Rev. Sci. Instrum. **69**(2), 544 (1998).
[22]C. C. Speake, T. J. Quinn, R. S. Davis, and S. J. Richman, "Experiment and theory in anelasticity," Meas. Sci. Technol. **10**(6), 430 (1999).